Single-Cell Transcriptomic Sequencing Reveals Tissue Architecture and Deciphers Pathological Reprogramming During Retinal Ischemia in *Macaca fascicularis*

Lin Li,[1,2] Sipeng Zuo,[1,2] Yan Liu,[1,2] Ludi Yang,[1,2] Shengfang Ge,[1,2] Fuxiang Ye,[1,2] Peiwei Chai,[1,2] and Linna Lu[1,2]

[1]Department of Ophthalmology, Ninth People's Hospital, Shanghai Jiao Tong University School of Medicine, Shanghai, People's Republic of China
[2]Shanghai Key Laboratory of Orbital Diseases and Ocular Oncology, Shanghai, People's Republic of China

Correspondence: Fuxiang Ye, Department of Ophthalmology, Ninth People's Hospital, Shanghai Jiao Tong University School of Medicine, Shanghai 200025, People's Republic of China; yefux@sjtu.edu.cn.
Peiwei Chai, Department of Ophthalmology, Ninth People's Hospital, Shanghai Jiao Tong University School of Medicine, Shanghai 200025, People's Republic of China; chaipeiwei123@sjtu.edu.cn.
Linna Lu, Department of Ophthalmology, Ninth People's Hospital, Shanghai Jiao Tong University School of Medicine, Shanghai 200025, People's Republic of China; linatutu@sjtu.edu.cn.

L. Li, S. Zuo, and Y. Liu contributed equally to this work.

Received: August 31, 2023
Accepted: December 27, 2023
Published: January 12, 2024

Citation: Li L, Zuo S, Liu Y, et al. Single-cell transcriptomic sequencing reveals tissue architecture and deciphers pathological reprogramming during retinal ischemia in *Macaca fascicularis*. *Invest Ophthalmol Vis Sci.* 2024;65(1):27. https://doi.org/10.1167/iovs.65.1.27

Purpose. Acute retinal arterial ischemia diseases (ARAIDs) are ocular emergencies that require immediate intervention within a restricted therapeutic window to prevent blindness. However, the underlying molecular mechanisms contributing to the pathogenesis of ARAIDs remain enigmatic. Herein, we present the single-cell RNA sequencing (scRNA-seq) alterations during ischemia in the primate retina as a preliminary endeavor in understanding the molecular complexities of ARAIDs.

Methods. An ophthalmic artery occlusion model was established through ophthalmic artery ligation in two *Macaca fascicularis*. scRNA-seq and bioinformatics analyses were used to detect retinal changes during ischemia, which are further validated by immunofluorescence analysis. Western blot and flow cytometry assays were performed to measure the microglia polarization status.

Results. The findings of this study reveal notable changes in the retina under acute ischemic conditions. Particularly, retinal ischemia compromised mitochondrial functions of rod photoreceptors, partly leading to the rapid loss of healthy rods. Furthermore, we observed a noteworthy transcriptional alteration in the activation of microglia induced by ischemia. The targeted correction of the proinflammatory cytokine CXCL8 effectively suppresses microglia M1 polarization in retinal ischemia, ultimately reducing the proinflammatory transformation in vitro. In addition, retina ischemia induced the apoptotic inclination of endothelial cells and the heightened interaction with microglia, which signifies the influence of microglia in disrupting the retinal–blood barrier.

Conclusions. Our research has successfully identified and described the pathologic alterations occurring in several cell types during a short period of ischemia. These observations provide valuable insights for ameliorating retinal damage and promoting the restoration of vision.

Keywords: acute retinal arterial ischemia diseases, *macaca fascicularis*, single-cell RNA sequencing

The primate retina exhibits a remarkably elevated energy requirement, which is supported by a specialized blood supply. The presence of a restricted intraretinal blood vessel network, in conjunction with a robust choriocapillaris, facilitates unimpeded light transmission and visual functions.[1] Insufficient blood supply due to blocked intraretinal vessels or degenerative choriocapillaris can lead to uncontrolled angiogenesis, resulting in various retinal diseases such as diabetic retinopathy, age-related macular degeneration, and retinal ischemia diseases.[2] Although the mechanical changes associated with diabetic retinopathy and age-related macular degeneration have been elucidated through single-cell transcriptomic analysis, the exploration of arterial occlusive disease in this context remains unexplored.

Notably, acute retinal arterial ischemia diseases (ARAIDs) represent urgent ocular emergencies leading to blindness, necessitating prompt intervention within a limited therapeutic time frame of approximately 4 to 6 hours, including ophthalmic artery occlusion, central retinal arterial occlusion, and branch retinal arterial occlusion.[3,4] The characteristic features of ARAIDs are typically identified as initial visual

acuity of 20/400 or worse, as well as a lack of visual acuity improvement compared to nonischemic cases.[5] In addition to abrupt vision loss, the available therapeutic interventions for ARAIDs are currently limited and yield minimal effectiveness in terms of enhancing visual acuity.[6] Therefore, it is imperative and time-sensitive to elucidate the mechanism during the acute ischemic period, as this may extend the therapeutic time window and optimize the restoration of visual acuity and visual field to the greatest extent possible.

ARAIDs, combined with the acute interruption of blood flow, are often caused by the emboli from the circulation and lead to irreversible retinal damage within a few hours.[7] Despite its high risk of blindness, analyses are often made from the perspective of epidemiology and clinical feature, leaving the molecular mechanisms underlying the pathologic programming largely unresolved.[8] Therefore, the remarkable alterations in the retinal microenvironment observed in ARAIDs remain largely unexplored, and the systemic landscape underlying ARAIDs remains enigmatic.

Herein, we initially present the single-cell RNA sequencing (scRNA-seq) alterations during ischemia in primate retina. Our study elucidates the alterations in the retina during acute ischemic conditions, characterized by substantial functional damages in rod photoreceptors and endothelial cells, as well as pronounced activation and accumulation of microglia. Our study has identified and characterized the pathologic changes in various major cells during a brief ischemic period and has also proposed a potential target for mitigating retinal damage and facilitating vision restoration.

Methods

Macaca Fascicularis

This study involved two male macaques, aged 8 and 9 years, respectively. The macaques were acquired from and housed and operated on at the Ninth People's Hospital, Shanghai Jiao Tong University School of Medicine. All procedures involving primates were granted approval by the Institutional Animal Care and Use Committee of the Ninth People's Hospital, Shanghai Jiao Tong University School of Medicine (grant number: PL22-0871) and handled according to the ARVO Statement for the Use of Animals in Ophthalmic and Vision Research.

Ophthalmic Artery Occlusion and Retina Ischemia

Prior to the surgical procedure, anesthesia was administered, and the body's core temperature was diligently monitored and regulated. The macaques were anesthetized for the entire operation. The eyelids were delicately extended, and the lateral walls of the orbit were dissected, with careful dissection of the muscles and blood vessels until complete exposure of the posterior region of the eyeball was achieved. In front of the common tendinous ring, an artery travels alongside the optic nerve and gives off branches along its course. The ophthalmic artery was ligated for 6 hours near the common tendinous ring where the short posterior ciliary arteries have not arisen. A macaque was randomly selected for bilateral ligation with two retinas used for single-cell analysis. A portion of each retina was preserved for immunofluorescence analysis. The other macaque that underwent the sham operation experienced the same surgical procedure without ligation, and the allocation of the two retinas was the same as with the ligation one.

Single-Cell Suspension

Fresh retinas from two separate macaques were promptly isolated under the operating microscope and preserved in the sterile ice-cold Tissue Preservation Solution (Singleron, Nanjing, China) buffer. The samples underwent a triple wash with Hanks' Balanced Salt Solution and were subsequently digested using 2 to 3 mL Tissue Dissociation Solution (Singleron) at a temperature of 37°C. The digestion process involved gentle pipetting for a duration of 15 minutes until the absence of any discernible tissue blockage. The solution was subsequently subjected to centrifugation at $350 \times g$ for a duration of 5 minutes and gently resuspended using phosphate-buffered saline. Ultimately, the samples were stained with trypan blue (Sigma, St. Louis, MO, USA) and the viability of the cells was assessed through microscopic examination.

Library Preparation and scRNA-Seq

Single-cell suspensions at the concentration of 1×10^5 cells/mL were loaded into microfluidic devices and scRNA-seq was processed through the 10X Genomics (Pleasanton, CA, USA) Chromium platform. After lysing and being marked with specific barcode and unique molecular identifier (UMI), RNA was released and reverse-transcribed into cDNA. Subsequently, the scRNA-seq libraries were constructed based on the processed cDNA. Individual libraries were diluted to 4 nM and pooled for sequencing. Last, pools were sequenced on Illumina (San Diego, CA, USA) HiSeq X with 150-bp paired end reads.

scRNA-seq Quantifications and Statistical Analysis

Raw reads were processed to generate gene expression profiles using an internal pipeline. Depending on the barcode, UMI, and gene, reads were grouped to calculate the number of UMIs of genes in each cell. The UMI count tables of each cellular barcode were employed for further analysis. Seurat R package (version 4.1.0) and Cellranger (10X Genomics) were applied for raw data pretreatment and quality control. Cells with more than 200 genes and less than 20% mitochondrial reads were retained for further analysis. STAR (Spliced Transcripts Alignment to a Reference, version 2.6.1) was used to align reads to the *Macaca fascicularis* reference genome (Ensembl 100, 2020). The mean gene number and mean transcript of control retina were 913.90 and 1767.88, respectively. Meanwhile, the mean gene number and mean transcript of ischemic retina were 1035.82 and 2190.91, respectively. Cell-type identification and clustering analysis were performed by the Seurat program (version 4.1.0), and parameter resolution to 0.6 was set for clustering analyses. Afterward, differentially expressed genes (DEGs) between different samples or clusters were identified by the Seurat program (version 4.1.0) with the standard of $|\log_2(\text{fold change})| > 0.5$ and $P < 0.05$. Furthermore, Gene Ontology (GO), Kyoto Encyclopedia of Genes and Genomes (KEGG), and REACTOME function enrichment analysis were carried out on the gene set using the clusterProfiler (version 4.6.2), and pseudotime analyses were carried out using monocle2 (version 2.26.0). The cell-to-cell communication analyses were carried out using CellChat (version 1.6.1) to quantify the specific ligand–receptor interaction between cell populations.[9]

Investigative Ophthalmology & Visual Science

Cell Culture

The mouse microglia BV2 cell line was purchased from China Center for Type Culture Collection (Wuhan, China), and a short tandem repeat analysis was conducted to verify the genuineness of the cell line, confirming its identity as BV2. BV2 cell line was cultured in RPMI 1640 medium (Invitrogen, Carlsbad, CA, USA) supplemented with 10% fetal bovine serum (Gibco, GrandIsland, NY, USA), 1% glutamine, and 1% penicillin/streptomycin under the standard conditions. Cells were seeded in six-well plates at 5×10^5 cells/well for 24 hours and treated with 100 ng/mL Lipopolysaccharide (LPS) (Selleck Chemicals, Houston, TX, USA) and indicated concentration of reparixin (Selleck Chemicals) for another 24 hours.[10]

Western Blotting

BV2 cells were washed and lysed in lysis buffer containing proteinase inhibitors (87785; Thermo Fisher Scientific, Waltham, MA, USA) on ice. We used 15 µg of each protein sample for Western blotting. The protein samples were then resolved by SDS-PAGE and transferred to PVDF membranes (Millipore, Burlington, MA, USA) in order. The 10% milk was used next to block the membrane for 2 hours at room temperature. Then, primary antibodies were incubated with the membrane: anti-CD86 (ab239075; Abcam, Cambridge, MA, USA), anti-COX2 (ab179800; Abcam), anti–IL-10 (60269-1-Ig; Proteintech, Wuhan, China), and anti-GAPDH (60004-1-Ig; Proteintech). After removal of primary antibodies and being washed, the membranes were incubated with horseradish peroxidase–conjugated secondary antibodies (SA00001-1, SA00001-2; Proteintech) for 2 hours at room temperature. After being washed, immunoreactive bands were visualized using the ECL kit and the detection instrument. These experiments were performed in triplicate, and we did not apply any masking methodology for this experiment.

Flow Cytometry

Flow cytometry was used in order to assess the expression of CD86 and IL-10 in BV2 cells. BV2 cells were seeded in triplicate onto six-well plates at 2.5×10^5 cells/well for 24 hours and treated with 100 ng/mL LPS and reparixin in a concentration gradient. Cells were then collected, resuspended into the cell suspension at the appropriate concentration, and incubated with APC anti-CD86 (105011; BioLegend, San Diego, CA, USA) and PE anti–IL-10 (505007; BioLegend) in the dark room for flow cytometry. The cell suspension was subjected to Cytoflex S flow cytometry (Beckman, Brea, CA, USA) and analyzed by CytoExpert software (Beckman). These experiments were performed in triplicate without masking.

Immunofluorescence

A portion of each retina was used for immunofluorescence. The retina from the ligated macaque was in comparison with the one from the macaque that underwent the sham operation. Fixed retinal tissues were embedded, cut into 2-µm-thick sections, and fixed on the polylysine-coated slides at 60°C for 30 minutes. After being washed three times, the sections were blocked with normal goat serum (Gibco) at room temperature for 2 hours. After being washed twice, the samples were incubated with anti–IBA-1 (66827-1-Ig; Proteintech), anti-INOS (ab283655; Abcam), anti-CD206 (ab64693; Abcam), or anti–Cleaved Caspase-8 (8592T; Cell Signaling Technology, Danvers, MA, USA) antibody at 4°C for 12 hours. After being washed three times, the tissues were incubated with fluorescent secondary antibodies for 2 hours at room temperature. The images were acquired using the fluorescence microscope.

Results

Single-Cell Transcriptome Depiction of Macaque Retinas and Identification of Major Cell Types

Cell alterations of the ischemic macaque retina were generated through droplet-based scRNA-seq following 6 hours of ophthalmic artery occlusion by operation (Fig. 1A). A total of 9495 cells from four retinas, two from the ischemic group and two from the control group, were collected for high-quality cell atlases following quality inspection. The initial analysis of the single-cell transcriptome data involved categorizing similar individual cells into specific cell subpopulations based on their gene expression profiles, utilizing the uniform manifold approximation and projection (UMAP) technique.[11] The cells were categorized into 13 primary classes using the widely recognized retina cell types and the firmly established gene signatures specific to each class[12,13] (Figs. 1B, 1C). In this study, we have assigned cell identities to various cell types with the retina based on the expression of hallmark genes, including rod photoreceptors (PDE6A, GNGT1, RHO), cone photoreceptors (ARR3, PDE6H, GUCA1C), bipolar cells (VSX2, LRTM1, TRPM1), horizontal cells (LAMP5, SLC6A9, CPLX3), amacrine cells (GAD1, C1QL2, AMIGO2), retinal ganglion cells (SNCG, NEFM, SLC17A6), microglia (C1QA, C1QB, CD163), astrocytes (GPX3, WIF1, FRZB), Müller cells (TTR, RDH5, ENPP2), pericytes (RGS5, CALD1, ACTA2), endothelial cells (CLDN5, ITM2A, RNASE1), neutrophils (S100A8, S100A9, CSF3R), and T cells (GZMB, CCL5, CD3D). The expression of these selected marker genes is depicted in dot plots (Fig. 1D).

Rod Photoreceptors Experienced Rapid Loss With Metabolic Reprogramming

In order to ascertain the retinal cell populations impacted by ischemic change, we conducted a comparative analysis of the proportions and communications of various cell clusters in retinas (Figs. 2A, 2B and Supplementary Fig. S1). The visual transduction pathway, situated within the retina, consists of various components, including the rod photoreceptor, cone photoreceptor, bipolar cell, horizontal cell, amacrine cell, and retinal ganglion cell (Fig. 2C).[14] Based on the analysis of cellular communication, a notable decline in rod-interacting cells has been observed, accompanied by a prominent rise in microglia-interacting frequencies. Notably, the healthy rod exhibits the most substantial reduction in comparison, while the proportions of the cone, horizontal cell, and amacrine cell did not present with remarkable alteration (Fig. 2D). Meanwhile, the ischemic retina shows more cleaved caspase 8 signal in the outer nuclear layer, consistent with the reduction of detected healthy rod photoreceptors in single-cell sequencing (Supplementary Fig. S2). Rod photoreceptors, as the major executor of scotopic vision,[15] have a degenerated change compared with the normal groups.

In order to delve deeper into the heterogeneity underlying the reduction, trajectory analyses were conducted on

Investigative Ophthalmology & Visual Science

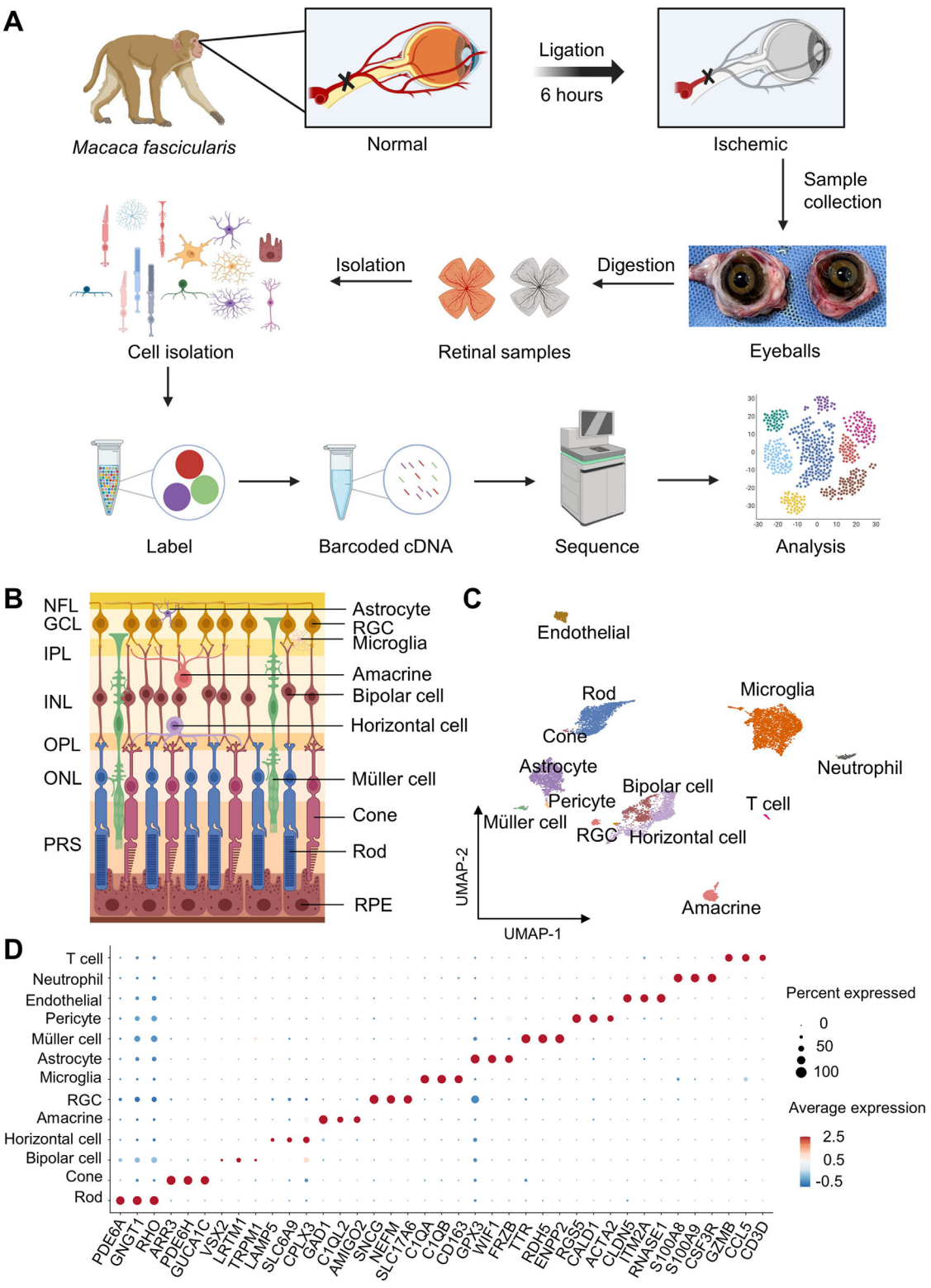

Figure 1. Single-cell profiling of retinal ischemia model. (**A**) Experimental and data analysis workflow for inducing macaque retinal ischemia (*top*) and scRNA-seq (*bottom*). The ophthalmic artery was ligated for 6 hours for model construction. (**B**) Sketch of retinal architecture showing its major cell classes, including retinal ganglion cell (RGC), astrocyte, microglia, amacrine, bipolar cell, horizontal cell, Müller cell, rod and cone photoreceptors, and retinal pigment epithelium cell (RPE) with their position in eight major retinal layers. (**C**) UMAP representation of macaque major retinal classes labeled with cell types. (**D**) Gene expression dot blot showing the specific marker genes (*columns*) across all clusters (*rows*).

Investigative Ophthalmology & Visual Science

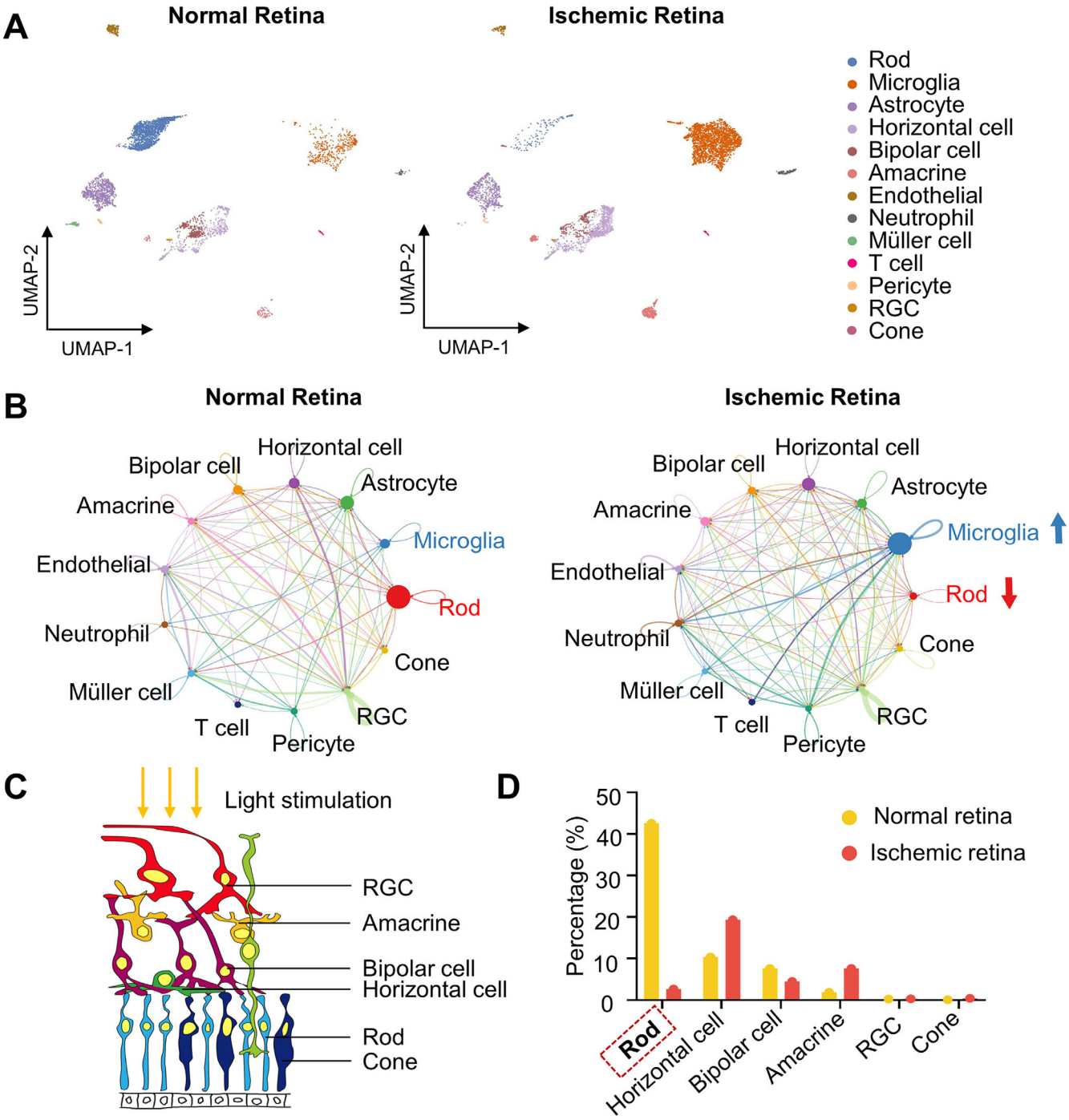

Figure 2. Comparison of single-cell transcriptome profiles between normal and ischemic retina. (**A**) UMAP representation of single cells from normal and ischemic retina labeled with cell types. (**B**) Network view of cell-to-cell communications within normal and ischemic retinas showing the enhanced communication of microglia and weakened communication of rod photoreceptor under ischemic conditions. (**C**) Sketch of retinal cross section showing cells participating in the visual transduction pathway under light stimulation. (**D**) Bar graph showing the percentage of each visual transduction-related subset within the normal and ischemic retina.

clusters of rod photoreceptors. These analyses revealed five developmental hierarchies and a binary branched structure: cluster 1 serving as the root, clusters 2 to 4 representing the end state of branch 1 and consisting of predominantly normal clusters, and cluster 5 representing the end state of branch 2 and primarily comprising ischemic group cells (Figs. 3A–C). Notably, the developmental trajectory of rod photoreceptors from ischemic and normal samples was distinctly different. We identified the DEGs between two branches in the next step. KEGG and REACTOME analyses showed an active metabolic activity in states 2 to 4 compared with the other rod photoreceptor, including generating metabolites and ATP to supply more vigorous protein synthesis and respiration, indicating high demand of energy (Figs. 3D, 3E). In comparison to other groups, the ischemic dominant group exhibited an upregulation of

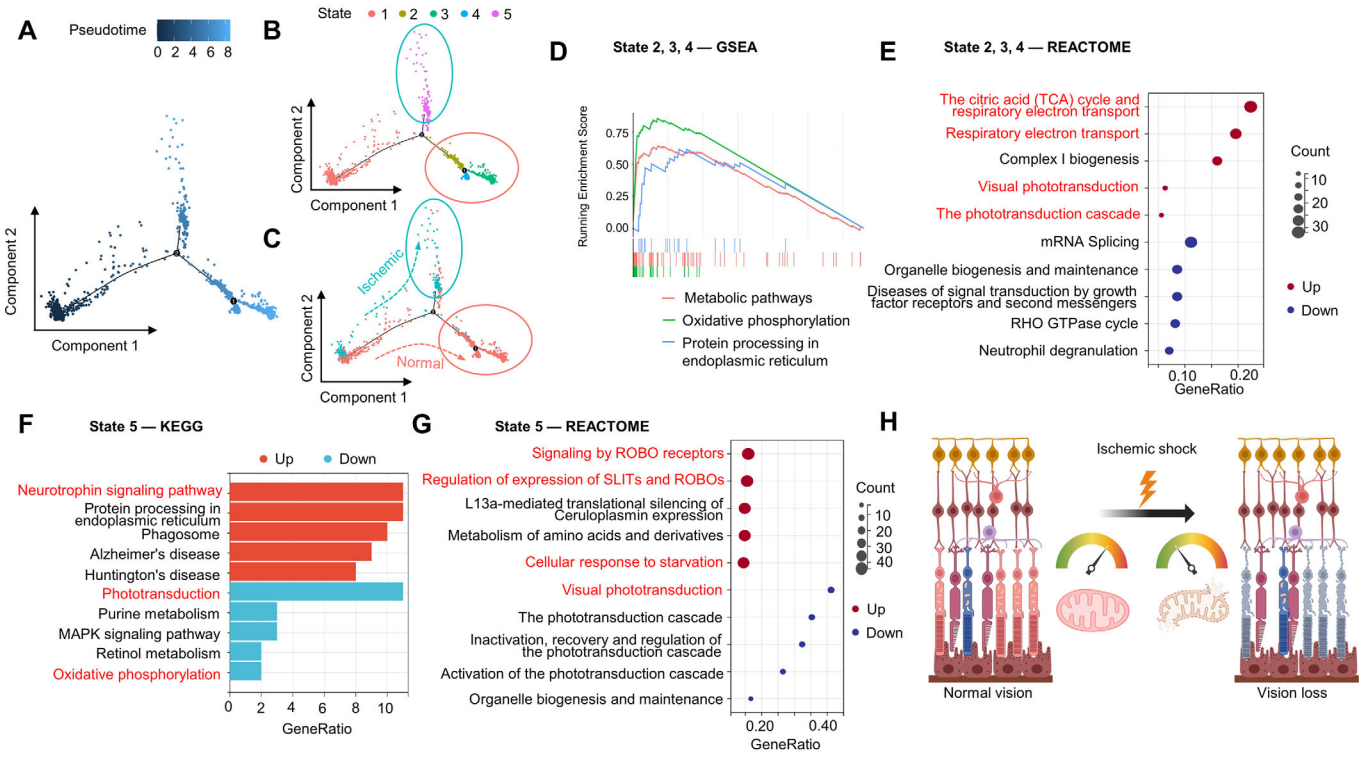

Figure 3. Transcriptional and functional alternations of rod photoreceptor subtypes. (**A–C**) Trajectory analyses showing the pseudotime (**A**), state (**B**), and sample resources (**C**) of rod photoreceptor cluster. *Arrow* indicates the pseudotime of two branches from early ones to late ones. (**D**) gene set enrichment analysis (GSEA) showing the major altered pathways associated with DEGs in cell fate 1 cluster of rod photoreceptors. (**E**) Dot plots showing the REACTOME terms of upregulated (*red*) and downregulated (*blue*) DEGs in cell fate 1 cluster of rod photoreceptors. (**F**) Bar plots showing KEGG terms of upregulated (*red*) and downregulated (*blue*) DEGs in the cell fate 2 cluster of rod photoreceptors. (**G**) Dot plots showing the REACTOME terms of upregulated (*red*) and downregulated (*blue*) DEGs in the cell fate 2 cluster of rod photoreceptors. (**H**) Illustration showing the impact of metabolic activity on cell destiny during ischemic conditions. Rod photoreceptors with active mitochondria implying high energy demand were vulnerable to ischemia, while rod photoreceptors with comparative inactive mitochondria survived.

neurotrophin signaling pathways that were advantageous for the repair of ischemic tissue. Additionally, there was a downregulation of metabolic activity and phototransduction, which may partially explain the irreversible and progressive vision loss observed in clinical patients during the early stages[16–18] (Fig. 3F). REACTOME analysis of state 5 also revealed the ischemic dominant cluster expressed more signals to activate and polarize microglia such as slit glycoproteins and roundabout receptors[19] (Fig. 3G). Moreover, the metabolic disparities observed between the two branches suggest the susceptibility of regular rod photoreceptors, which require a substantial blood supply, to ischemic shock. Conversely, the ischemic groups exhibited a reduction in energy demand, enabling the survival of rod photoreceptors (Fig. 3H).

The Activation and Polarization of Microglia Plays an Important Role in Ischemic Shock

In the present study, as previously observed,[20] the retinal glia cells and the vasculature played a crucial role in providing metabolic and homeostatic support to neurons involved in visual transduction. Notably, our findings indicate the occurrence of homeostatic disequilibrium within a 6-hour time frame, characterized by microglia proliferation, immune cell aggregation, and endothelial apoptosis (Fig. 4A).

Microglia, as a key regulator of immunologic homeostasis,[21] exhibited substantial proliferation (Fig. 4B) and biphasic polarization in the ischemic group, with a ratio of 2:3 in M1 and M2 clusters (Figs. 4C–E). The robust proliferation of cells could be demonstrated by conducting a KEGG analysis on quiescent microglia, which revealed an upregulation of pathways related to organelle fission and nuclear division (Supplementary Fig. S3A). The presence of two distinct states of microglia was confirmed through immunofluorescent staining and heatmap (Fig. 4F). In order to gain a deeper understanding of these two polarized states, we performed functional analyses using GO approaches. As depicted in Supplementary Figure S3B, the M1 phenotypic polarization exerted a favorable influence on the activation and augmentation of the immune system and inflammation across various dimensions. In stark contrast, the M2 phenotypic polarization exhibited a distinctly different impact, as evidenced by the downregulation of molecular functions conducive to immune activation (Supplementary Fig. S3C). The M2 phenotype also showed the characteristics of enhanced glucose metabolism, protein processing, and maturation, which may beneficial to the tissue repair.

CXCL8 Repression Shifts the Retinal Microglia M1/M2 Phenotypic Polarization In Vitro

The deleterious effects of the excessive M1 phenotype microglia on ischemic tissue repair, characterized by heightened immune response and inflammation, have been widely

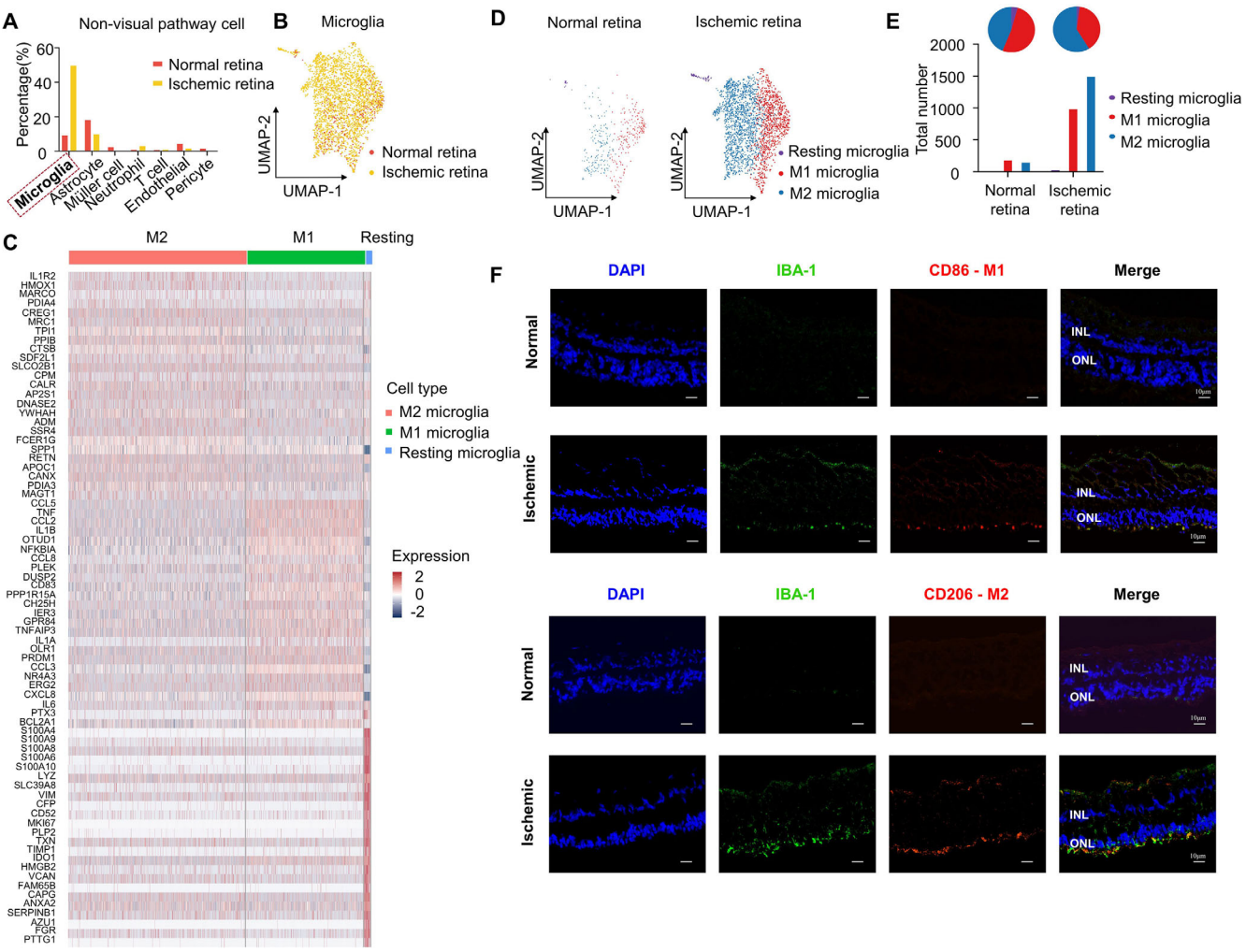

Figure 4. Activation and polarization of microglia under ischemic condition. (**A**) Bar graph showing the percentage of each nonvisual pathway subset within the normal and ischemic retina. (**B**) UMAP representation of microglia cluster labeled with samples. (**C**) Heatmap showing the different expressed genes (*rows*) of the three subpopulations of microglia (*columns*) with different colors representing its intensity. (**D**) UMAP representation of normal retina (*left*) and ischemic retina (*right*) labeled with polarization state. (**E**) Bar graph and pie chart showing the number and proportion of resting, M1 and M2 microglia in normal and ischemic retinas. (**F**) Images of multiplex in situ hybridization with immunofluorescence showing the M1 (IBA-1$^+$/CD86$^+$) and M2 (IBA-1$^+$/CD206$^+$) microglia in normal and ischemic retinas. *Scale bar*: 10 µm.

acknowledged.[22] Conversely, the M2 phenotype has been recognized as potentially advantageous.[23] Recent research has increasingly demonstrated the benefits of promoting M2 polarization in mitigating ischemic injury.[24,25] In this study, a total of 848 genes were identified as DEGs when comparing resting microglia to the M1 phenotype. Additionally, 20 DEGs were observed when comparing the M1 phenotype to the M2 phenotype. Notably, 15 DEGs were found to be present in both clusters (Supplementary Fig. S4A and Supplementary Table S1). Among these genes, *CXCL8* was selected as a potential target due to its substantial fold change in the comparison between the M1 phenotype and resting microglia (Fig. 5A). In comparison to the M2 phenotype, the M1 phenotype exhibited a higher expression of *CXCL8* (Supplementary Fig. S4B). The feature plots and violin plots effectively illustrated the expression level and distribution of *CXCL8* in microglia clusters from two samples, highlighting the elevated expression in the ischemic cluster (Figs. 5B, 5C).

To establish the association between *CXCL8* expression and microglia polarization, our study employed reparixin, a targeted inhibitor of CXCL8 receptor.[26] Importantly, the combination of LPS and reparixin reduced the protein levels of M1 markers (COX2, CD86) and increased the protein expression of the M2 marker (IL-10) in BV2 cells, with the effect being dependent on the concentration of reparixin (Fig. 5D). Furthermore, the findings derived from flow cytometry analysis (Fig. 5E) demonstrated a consistent pattern in the M2 phenotypic polarization of BV2 cells upon stimulation with LPS and a substantial higher level of the M2/M1 ratio (Fig. 5F). Notably, an increase in reparixin concentration corresponded to a decrease in the polarization ratio of the M1 phenotype, accompanied by an elevated M2/M1 ratio. These results provide substantial evidence supporting the crucial involvement of CXCL8 in the polarization process, wherein its repression can effectively modulate microglia M1/M2 polarization.

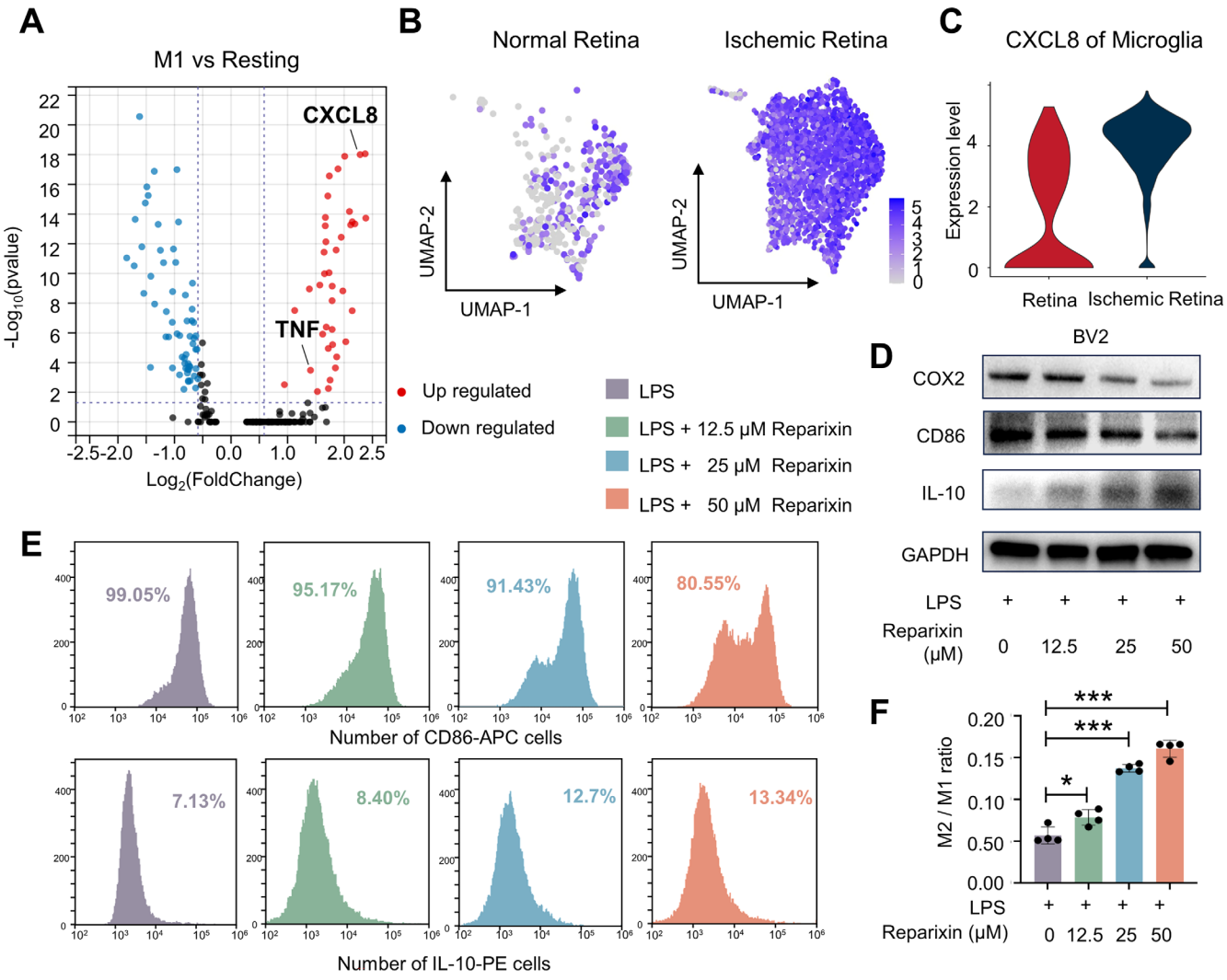

Figure 5. CXCL8 inhibition facilitates M2 microglia polarization. (**A**) Volcano plot showing all DEGs between resting phenotypic and M1 phenotypic microglia with the label of CXCL8 and TNF. (**B**, **C**) UMAP representation and violin plot showing distribution and expression levels of *CXCL8* in different microglia clusters. (**D**) Western plotting showing the expression of BV2 cells M1 markers (COX2, CD86) and M2 marker (IL-10) in the LPS, LPS + 12.5 μM reparixin, LPS + 25 μM reparixin, and LPS + 50; μM reparixin groups. (**E**) Flow cytometry showing the proportion of $CD86^+$ (M1) and $IL\text{-}10^+$ (M2) BV2 cells in LPS-induced BV2 cells. (**F**) Statistical analysis of the M2/M1 ratio in LPS, LPS + 12.5 μM reparixin, LPS + 25 μM reparixin, and LPS + 50 μM reparixin groups. The data are presented as the mean ± SD. Significance was determined by an unpaired two-tailed Student's *t*-test. $^{***}P < 0.001$.

Pathologic Changes of Endothelial Cells During the Acute Ischemic Period

The alterations in the retinal microenvironment, particularly changes in endothelial cells, play a crucial role in the accumulation of immune-related or inflammatory cells.[27] The GO analysis of the entire ischemic endothelial population highlights the apoptotic tendency, characterized by the upregulation of multiple apoptotic signaling pathways and the downregulation of adhesion molecules. As endothelial and its tight junction forms a key part of blood–retinal barrier (BRB) integrity,[28] this suggests a disruption of the blood–retinal barrier, as depicted in Figure 6A. Consistently, the downregulation of tight junction marker (ZO-1 and occludin) in endothelial cells showed the BRB dysfunction after retinal ischemia (Fig. 6B). Moreover, the augmented intercellular communication exhibited by microglia suggests the presence of endothelial dysfunction and disruption of the BRB, analogous to the blood–brain barrier[29] (Fig. 6C).

Discussion

During the acute ischemic period, substantial alterations occur in the retina. This study aimed to create a model of ischemic retina in *M. fascicularis* and identify key characteristics of compromised primate retina homeostasis. These characteristics include the rapid depletion of healthy rod photoreceptors accompanied by heightened metabolic activity, the aggregation of functional microglia with bilateral polarization, and the apoptosis of endothelial cells, indicating the disruption of the inner BRB. Furthermore, the proinflammatory polarization of microglia can be impeded through the repression of *CXCL8*, which was selected as a target based on sequencing data. In this study, we present the initial transcriptomic atlas of the acute ischemic retina,

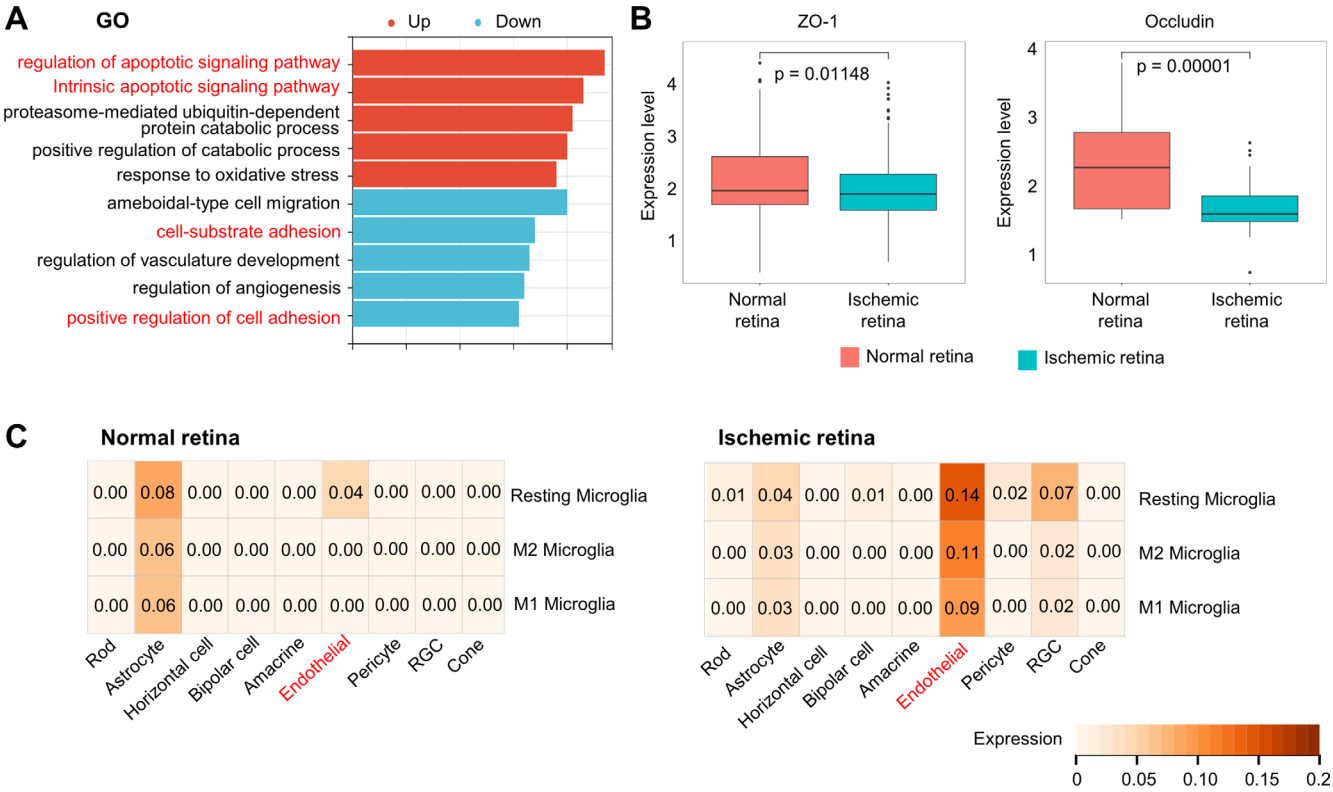

Figure 6. Pathologic changes of endothelial cells under the ischemic condition. (**A**) Bar plots showing GO terms of upregulated (*red*) and downregulated (*blue*) DEGs in the ischemic endothelial group compared with the normal group. (**B**) Bar plots of tight junction marker expression in endothelial cells from normal and ischemia retinas. Significance was determined by an unpaired two-tailed Student's *t*-test. Nominal, uncorrected *P* value for ZO-1: 0.01148; nominal, uncorrected *P* value for occludin: 0.00001. (**C**) Visualization and quantification of intercellular communication between microglia subtypes and other major retinal cells.

offering novel insights into the distinct responses of various retinal cells to the rapid decrease in blood flow. Additionally, our findings contribute to the development of potential therapeutic interventions for vision restoration, particularly with an extended therapeutic window.

The rapid depletion of blood supply results in rapid onset of visual impairment and blindness.[30] Our study has identified that the metabolic reprogramming of rod photoreceptors during the early stages may be accountable for this vision loss. Furthermore, a separate study has provided evidence indicating that the malfunction and disturbance of photoreceptor mitochondria manifest within 8 hours of acute energy depletion, resulting in irreversible cellular demise.[31] This finding is consistent with our own observation that retinal ischemia in rod cells diminishes aerobic respiration. Therefore, restoring mitochondrial function to enable metabolic circulation in rod photoreceptors holds promise as a therapeutic strategy for acute retinal artery ischemic diseases.

Microglia are commonly recognized as playing a crucial pathogenic role in ischemic disorders, with its states being categorized into the proinflammatory M1 state and the anti-inflammatory M2 state.[32] Additionally, it has been documented that diverse macrophage populations express both M1 and M2 markers, enabling a rapid transition between functional phenotypes.[33,34] This study reveals the presence of intense activation and biphasic polarization of microglia in the ischemic retina. A similar numerical pattern of M1 and M2 phenotypic polarization was observed in acute ischemic cerebral tissue.[35] Meanwhile, we supposed that the microglia in the ischemic retina is composed of the circulating migration and local cell division, which needs to be studied further, such as using GFP-labeled bone marrow transplantation,[36] to uncover the source of the increased immune cells. The activation and polarization of microglia toward the M2 phenotype is advantageous for the recovery from ischemic diseases, such as cerebral ischemia.[37,38] In this study, we have identified CXCL8, a proinflammatory cytokine, as a target for suppressing M1 polarization in retinal ischemia, resulting in a reduction of proinflammatory transformation in LPS-activated microglia.

Furthermore, the heightened apoptotic inclination of endothelial cells, the downregulated tight junction of endothelial cells, and the augmented interaction with microglia indicate the potential role of microglia in the disruption of the blood barrier in the early stages of the condition.[39,40] A separate study provided direct evidence of the impairment of the retinal endothelial barrier through the measurement of electrical parameters of barrier integrity under cytopathic hypoxia in an in vitro setting.[41] Taken together, these aforementioned findings imply the presence of BRB dysfunction in the initial phase of ischemic retinopathy. Moreover, research has demonstrated that inhibiting endothelial apoptosis promotes revascularization in the ischemic retina.[42] Additionally, targeting caspase 9, an apoptosis activator in endothelial cells, has been shown to mitigate the edema and inflammation resulting from vessel occlusion.[43] Furthermore, the activation of microglia has been found to influence blood barrier integrity, depending on its polarization states.[44,45] Consequently, directing

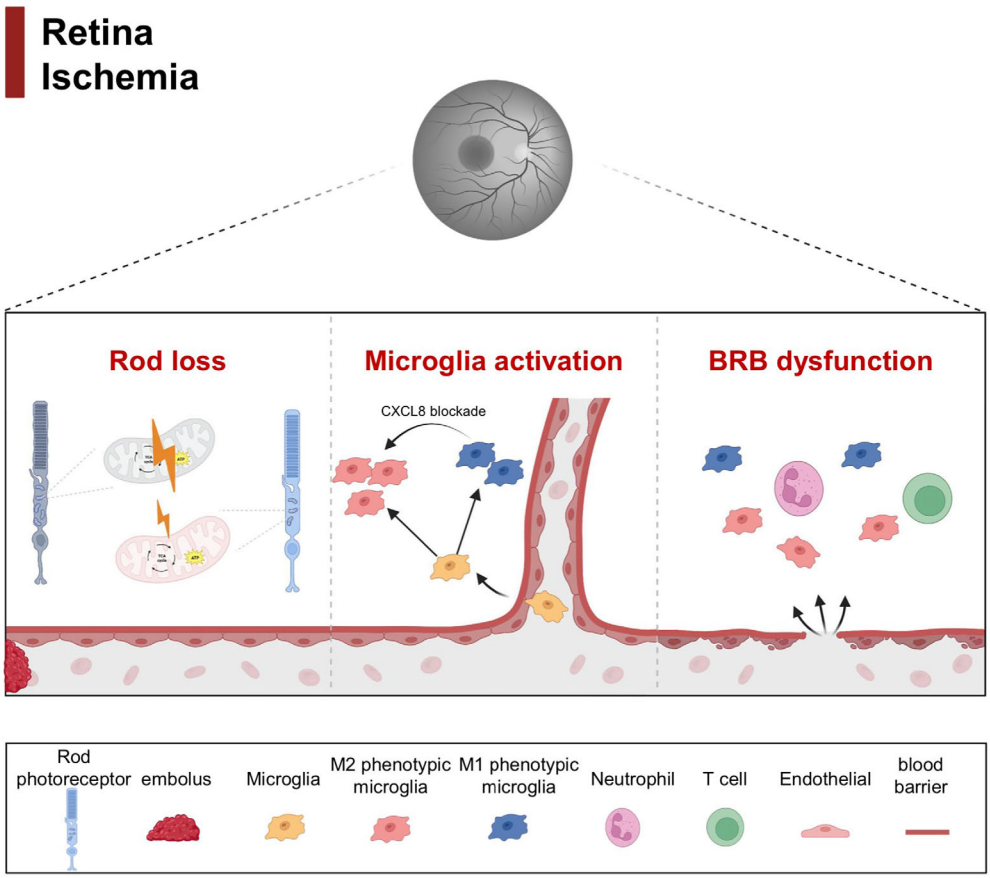

Figure 7. Illustration of pathologic alternations in retina during acute ischemia. Schematic diagram of retinal microenvironment in normal and ischemic conditions showing the rapid loss of rod photoreceptors, functional impairments of endothelia, and the accumulation and polarization of microglia under ischemia, while the repression of CXCL8 resulted in beneficial M2 polarization.

interventions toward crucial regulators to ensure the survival of endothelial cells may offer a promising therapeutic approach to extend the therapeutic window.

In summary, our research has characterized the transcriptomic profile of the ischemic primate retina at the single-cell scale, shedding light on the alterations occurring during the early stages of retinal ischemia (Fig. 7). Specifically, we have identified that rods with activated mitochondrial functions are particularly susceptible to retinal ischemia. Furthermore, we have observed molecular changes in the adhesion molecules of endothelial cells, potentially contributing to the dysfunction of the blood–retina barrier. Additionally, we have discovered a novel regulator that enhances the beneficial effects of M2 phenotypic polarization, specifically in relation to microglia polarization.

Acknowledgments

Supported by the Science and Technology Commission of Shanghai Municipality (21ZR1437400, 23ZR1480100), the Cross-disciplinary Research Fund of Shanghai Ninth People's Hospital, Shanghai Jiao Tong University School of Medicine (JYLJ202211), the China Primary Health Care Foundation (No. CT202202100018), Shanghai Shenkang Hospital Development Center (SHDC2020CR2040B), National Natural Science Foundation of China (82373298, 82103240), Shanghai Key Clinical Specialty, Shanghai Eye Disease Research Center (2022ZZ01003), Shanghai Municipal Health Commission (GWVI-11.2-YQ19) and Shanghai Key Laboratory of Orbital Diseases and Ocular Oncology.

Data Availability Statement: The raw sequence data reported in this article have been deposited in the GEO (Gene Expression Omnibus) and NODE (The National Omics Data Encyclopedia) databases, under the accession number of GSE242229 and OEP004422, respectively.

Disclosure: **L. Li**, None; **S. Zuo**, None; **Y. Liu**, None; **L. Yang**, None; **S. Ge**, None; **F. Ye**, None; **P. Chai**, None; **L. Lu**, None.

References

1. Lejoyeux R, Benillouche J, Ong J, et al. Choriocapillaris: fundamentals and advancements. *Prog Retin Eye Res*. 2022;87:100997.
2. Campochiaro PA. Molecular pathogenesis of retinal and choroidal vascular diseases. *Prog Retin Eye Res*. 2015;49:67–81.
3. Biousse V, Nahab F, Newman NJ. Management of acute retinal ischemia: follow the guidelines! *Ophthalmology*. 2018;125:1597–1607.
4. Raber FP, Gmeiner FV, Dreyhaupt J, et al. Thrombolysis in central retinal artery occlusion: a retrospective observational study. *J Neurol*. 2023;270:891–897.
5. Hayreh SS. Ocular vascular occlusive disorders: natural history of visual outcome. *Prog Retin Eye Res*. 2014;41:1–25.
6. Hayreh SS. Central retinal artery occlusion. *Indian J Ophthalmol*. 2018;66:1684–1694.
7. Sharma RA, Dattilo M, Newman NJ, Biousse V. Treatment of nonarteritic acute central retinal artery occlu-

sion. *Asia Pac J Ophthalmol (Phila)*. 2018;7:235–241.
8. Lee D, Tomita Y, Yang L, Negishi K, Kurihara T. Ocular ischemic syndrome and its related experimental models. *Int J Mol Sci*. 2022;23:5249.
9. Jin S, Guerrero-Juarez CF, Zhang L, et al. Inference and analysis of cell-cell communication using CellChat. *Nat Commun*. 2021;12:1088.
10. Yang X, Xu S, Qian Y, Xiao Q. Resveratrol regulates microglia M1/M2 polarization via PGC-1α in conditions of neuroinflammatory injury. *Brain Behav Immun*. 2017;64:162–172.
11. Becht E, McInnes L, Healy J, et al. Dimensionality reduction for visualizing single-cell data using UMAP. *Nat Biotechnol*. 2019;37:38–44.
12. Yi W, Lu Y, Zhong S, et al. A single-cell transcriptome atlas of the aging human and macaque retina. *Natl Sci Rev*. 2021;8:nwaa179.
13. Peng YR, Shekhar K, Yan W, et al. Molecular classification and comparative taxonomics of foveal and peripheral cells in primate retina. *Cell*. 2019;176:1222–1237.e1222.
14. Voigt AP, Mullin NK, Stone EM, Tucker BA, Scheetz TE, Mullins RF. Single-cell RNA sequencing in vision research: insights into human retinal health and disease. *Prog Retin Eye Res*. 2021;83:100934.
15. Thoreson WB, Dacey DM. Diverse cell types, circuits, and mechanisms for color vision in the vertebrate retina. *Physiol Rev*. 2019;99:1527–1573.
16. Li Z, Wang H, Xiao G, et al. Recovery of post-stroke cognitive and motor deficiencies by Shuxuening injection via regulating hippocampal BDNF-mediated Neurotrophin/Trk signaling. *Biomed Pharmacother*. 2021;141:111828.
17. Schlecht A, Vallon M, Wagner N, Ergün S, Braunger BM. TGFβ-neurotrophin interactions in heart, retina, and brain. *Biomolecules*. 2021;11:1360.
18. Lee JS, Kim JY, Jung C, Woo SJ. Iatrogenic ophthalmic artery occlusion and retinal artery occlusion. *Prog Retin Eye Res*. 2020;78;100848.
19. Geraldo LH, Xu Y, Jacob L, et al. SLIT2/ROBO signaling in tumor-associated microglia and macrophages drives glioblastoma immunosuppression and vascular dysmorphia. *J Clin Invest*. 2021;131:e141083.
20. Kugler EC, Greenwood J, MacDonald RB. The "neuro-glial-vascular" unit: the role of glia in neurovascular unit formation and dysfunction. *Front Cell Dev Biol*. 2021;9:732820.
21. Rathnasamy G, Foulds WS, Ling EA, Kaur C. Retinal microglia—a key player in healthy and diseased retina. *Prog Neurobiol*. 2019;173:18–40.
22. Wang D, Liu F, Zhu L, et al. FGF21 alleviates neuroinflammation following ischemic stroke by modulating the temporal and spatial dynamics of microglia/macrophages. *J Neuroinflammation*. 2020;17:257.
23. Wang J, Xing H, Wan L, Jiang X, Wang C, Wu Y. Treatment targets for M2 microglia polarization in ischemic stroke. *Biomed Pharmacother*. 2018;105:518–525.
24. Liu X, Liu J, Zhao S, et al. Interleukin-4 is essential for microglia/macrophage M2 polarization and long-term recovery after cerebral ischemia. *Stroke*. 2016;47:498–504.
25. Li L, Gan H, Jin H, et al. Astragaloside IV promotes microglia/macrophages M2 polarization and enhances neurogenesis and angiogenesis through PPARγ pathway after cerebral ischemia/reperfusion injury in rats. *Int Immunopharmacol*. 2021;92:107335.
26. Lin C, He H, Liu H, et al. Tumour-associated macrophages-derived CXCL8 determines immune evasion through autonomous PD-L1 expression in gastric cancer. *Gut*. 2019;68:1764–1773.
27. Kovoor E, Chauhan SK, Hajrasouliha A. Role of inflammatory cells in pathophysiology and management of diabetic retinopathy. *Surv Ophthalmol*. 2022;67:1563–1573.
28. Li Y, Zou C, Chen C, et al. Myeloid-derived MIF drives RIPK1-mediated cerebromicrovascular endothelial cell death to exacerbate ischemic brain injury. *Proc Natl Acad Sci USA*. 2023;120:e2219091120.
29. Knopp RC, Banks WA, Erickson MA. Physical associations of microglia and the vascular blood-brain barrier and their importance in development, health, and disease. *Curr Opin Neurobiol*. 2022;77:102648.
30. Chen CS, Varma D, Lee A. Arterial occlusions to the eye: from retinal emboli to ocular ischemic syndrome. *Asia Pac J Ophthalmol (Phila)*. 2020;9:349–357.
31. Fan B, Li FQ, Zuo L, Li GY. mTOR inhibition attenuates glucose deprivation-induced death in photoreceptors via suppressing a mitochondria-dependent apoptotic pathway. *Neurochem Int*. 2016;99:178–186.
32. Hu X, Leak RK, Shi Y, et al. Microglial and macrophage polarization—new prospects for brain repair. *Nat Rev Neurol*. 2015;11:56–64.
33. Orihuela R, McPherson CA, Harry GJ. Microglial M1/M2 polarization and metabolic states. *Br J Pharmacol*. 2016;173:649–665.
34. Vogel DY, Vereyken EJ, Glim JE, et al. Macrophages in inflammatory multiple sclerosis lesions have an intermediate activation status. *J Neuroinflammation*. 2013;10:35.
35. Xiong XY, Liu L, Yang QW. Functions and mechanisms of microglia/macrophages in neuroinflammation and neurogenesis after stroke. *Prog Neurobiol*. 2016;142:23–44.
36. Caicedo A, Espinosa-Heidmann DG, Piña Y, Hernandez EP, Cousins SW. Blood-derived macrophages infiltrate the retina and activate Muller glial cells under experimental choroidal neovascularization. *Exp Eye Res*. 2005;81:38–47.
37. Wang Y, Jin H, Wang Y, et al. Sult2b1 deficiency exacerbates ischemic stroke by promoting pro-inflammatory macrophage polarization in mice. *Theranostics*. 2021;11:10074–10090.
38. Zhou S, Zhu W, Zhang Y, Pan S, Bao J. S100B promotes microglia M1 polarization and migration to aggravate cerebral ischemia. *Inflamm Res*. 2018;67:937–949.
39. Yun JH, Park SW, Kim KJ, et al. Endothelial STAT3 activation increases vascular leakage through downregulating tight junction proteins: implications for diabetic retinopathy. *J Cell Physiol*. 2017;232:1123–1134.
40. Shen H, Pei H, Zhai L, Guan Q, Wang G. Salvianolic acid C improves cerebral ischemia reperfusion injury through suppressing microglial cell M1 polarization and promoting cerebral angiogenesis. *Int Immunopharmacol*. 2022;110:109021.
41. El-Tanani S, Yumnamcha T, Singh LP, Ibrahim AS. Differential effects of cytopathic hypoxia on human retinal endothelial cellular behavior: implication for ischemic retinopathies. *Int J Mol Sci*. 2022;23:4274.
42. Grant ZL, Whitehead L, Wong VH, et al. Blocking endothelial apoptosis revascularizes the retina in a model of ischemic retinopathy. *J Clin Invest*. 2020;130:4235–4251.
43. Avrutsky MI, Ortiz CC, Johnson KV, et al. Endothelial activation of caspase-9 promotes neurovascular injury in retinal vein occlusion. *Nat Commun*. 2020;11:3173.
44. Kacimi R, Giffard RG, Yenari MA. Endotoxin-activated microglia injure brain derived endothelial cells via NF-κB, JAK-STAT and JNK stress kinase pathways. *J Inflamm (Lond)*. 2011;8:7.
45. Abcouwer SF, Shanmugam S, Muthusamy A, et al. Inflammatory resolution and vascular barrier restoration after retinal ischemia reperfusion injury. *J Neuroinflammation*. 2021;18:186.

Investigative Ophthalmology & Visual Science